

Nanofiber drawing and nanodevice assembly in poly(trimethylene terephthalate)

Xiaobo Xing, Yuqing Wang, and Baojun Li*

State Key Laboratory of Optoelectronic Materials and Technologies,
School of Physics and Engineering, Sun Yat-Sen University, Guangzhou 510275, China

*Corresponding author: stslbj@mail.sysu.edu.cn

Abstract: We report flexible and elastic enough nanofibers with diameters down to 60 nm and lengths up to 500 μ m, fabricated by one-step drawing process from molten poly(trimethylene terephthalate) (PTT), exhibiting high surface smoothness and length uniformity. A series of ultracompact devices (such as optical beam splitters, couplers, rings, resonators, and tweezer/scissor-shaped structures) and nanophotonic device arrays have been assembled by the PTT nanofibers. Quantitative studies demonstrate that the PTT nanofibers/nanofiber devices exhibit good guiding properties with low optical loss from visible to near infrared region. The results suggest that the PTT nanophotonic fibers/wires would be promising candidates in constructing miniaturized photonic devices and ultracompact photonic integrated circuits (PICs), and a one-step drawing as an alternative to the standard optical bench technique.

©2008 Optical Society of America

OCIS codes: (130.0130) Integrated optics; (130.3120) Integrated optics devices; (160.2290) Fiber materials; (220.4241) Nanostructure fabrication; (230.1150) All-optical devices; (310.6628) Subwavelength structures, nanostructures.

References and links

1. D. Appell, "Wired for success," *Nature* **419**, 553-555 (2002).
2. M. Law, D. J. Sirbuly, J. C. Johnson, J. Goldberger, R. J. Saykally, and P. Yang, "Nanoribbon waveguides for subwavelength photonics integration," *Science* **305**, 1269-1273 (2004).
3. L. Tong, R. R. Gattass, J. B. Ashcom, S. He, J. Lou, M. Shen, I. Maxwell, and E. Mazur, "Subwavelength-diameter silica wires for low-loss optical wave guiding," *Nature* **426**, 816-819 (2003).
4. L. Tong, L. Hu, J. Zhang, J. Qiu, Q. Yang, J. Lou, Y. Shen, J. He, and Z. Ye, "Photonic nanowires directly drawn from bulk glasses," *Opt. Express* **14**, 82-87 (2006).
5. J. C. Knight, G. Cheung, F. Jacques, and T. A. Birks, "Phase-matched excitation of whispering-gallery-mode resonances by a fiber taper," *Opt. Lett.* **22**, 1129-1131 (1997).
6. G. Brambilla, V. Finazzi, and D. J. Richardson, "Ultra-low-loss optical fiber nanotapers," *Opt. Express* **12**, 2258-2263 (2004).
7. G. Brambilla, F. Xu, and X. Feng, "Fabrication of optical fiber nanowires and their optical and mechanical characterisation," *Electron. Lett.* **42**, 517-518 (2006).
8. G. Brambilla, F. Koizumi, X. Feng, and D. J. Richardson, "Compound-glass optical nanowires," *Electron. Lett.* **41**, 400-402 (2005).
9. L. Tong, J. Lou, R. R. Gattass, S. He, X. Chen, L. Liu, and E. Mazur, "Assembly of silica nanowires on silica aerogels for microphotonic devices," *Nano Lett.* **5**, 259-262 (2005).
10. Y. Li, L. Tong, "Mach-Zehnder interferometers assembled with optical microfibers or nanofibers," *Opt. Lett.* **33**, 303-305 (2008).
11. S. A. Harfenist, S. D. Cambron, E. W. Nelson, S. M. Berry, A. W. Isham, M. M. Crain, K. M. Walsh, R. S. Keynton, and R. W. Cohn, "Direct drawing of suspended filamentary micro- and nanostructures from liquid polymers," *Nano Lett.* **4**, 1931-1937 (2004).
12. H. Liu, J. B. Edel, L. M. Bellan, H. G. Craighead, "Electrospun polymer nanofibers as subwavelength optical waveguides incorporating quantum dots," *Small* **2**, 495-499 (2006).
13. W. S. Lyoo, H. S. Lee, B. C. Ji, S. S. Han, K. Koo, S. S. Kim, J. H. Kim, J.-S. Lee, T. W. Son, and W. S. Yoon, "Effect of zone drawing on the structure and properties of melt-spun poly(trimethylene terephthalate) fiber," *J. Appl. Polym. Sci.* **81**, 3471-3480 (2001).
14. H. H. Chuah, "Orientation and structure development in poly(trimethylene terephthalate) tensile drawing," *Macromolecules* **34**, 6985-6993 (2001).

15. D. R. Kelsey, K. S. Kibler, and P. N. Tutunjian, "Thermal stability of poly(trimethylene terephthalate)," *Polymer* **46**, 8937-8946 (2005).
 16. C. Hwo, T. Forschner, R. Lowtan, D. Gwyn, and B. Cristea, "Poly(trimethylene phthalates or naphthalate) and copolymers: new opportunities in film and packaging applications," *J. Plastic Film & Sheeting* **15**, 219-234 (1999).
 17. H. H. Chuah and B. T. A. Chang, "Crystal orientation function of poly(trimethylene terephthalate) by wide-angle x-ray diffraction," *Polym. Bull.* **46**, 307-313 (2001).
 18. H. H. Chuah, "Intrinsic birefringence of poly(trimethylene terephthalate)," *J. Polym. Sci.: Part B: Polym. Phys.* **40**, 1513-1520 (2002).
 19. M. S. Khil, H. Y. Kim, M. S. Kim, S. Y. Park, and D.-R. Lee, "Nanofibrous mats of poly(trimethylene terephthalate) via electrospinning," *Polymer* **45**, 295-301 (2004).
 20. K. J. Kim, J. H. Bae, and Y. H. Kim, "Infrared spectroscopic analysis of poly(trimethylene terephthalate)," *Polymer* **42**, 1023-1033 (2001).
 21. C. J. Barrelet, A. B. Greytak, and C. M. Lieber, "Nanowire photonic circuit elements," *Nano Lett.* **4**, 1981-1985 (2004).
 22. F. Xu, P. Horak, and G. Brambilla, "Optical microfiber coil resonator refractometric sensor," *Opt. Express* **15**, 7888-7893 (2007).
 23. M. Sumetsky, "Optical fiber microcoil resonator," *Opt. Express* **12**, 2303-2316 (2004).
-

1. Introduction

The development of nanotechnology in photonics offers significant scientific and technological potentials [1,2]. It fosters the substantial efforts for exploring novel materials, developing easy fabrication techniques, reducing the size of photonic components, improving device integration density, and fabricating low-cost nanodevices. Since nanometer-scale photonic fibers/wires are highly desirable for applications in high density and miniaturized PICs, subwavelength-diameter wires have been drawn and demonstrated by flame-heated silica fiber [3] and bulk glasses [4] method. The method provides an easy and cheap photonic wires manufacturing technique, but a steady temperature distribution is required in the drawing region and the lengths of the fabricated wires are limited to 4 mm and tens of millimeters. Later, flame-brushing and microheater-brushing techniques were proposed to fabricate nanowires from silica fibers [5–7] and compound-glass fibers [8], respectively. The length of the fabricated nanowire is extended 110 mm, but this technique requires extremely good control of processing temperature and airflow around the nanowires. On the other hand, due to relatively low flexibility of silica and glasses, only wire-based simple devices such as 2×2 branch coupler [4,9], single-ring resonator [3,9], and single-Mach-Zehnder (MZ) interferometer [10] were assembled and demonstrated. Compared with silica and glasses, polymers have high flexibility, and thus can be arbitrarily bent/squeezed and molded to have variety of shapes [11,12]. As a promising polymer, PTT's trimethylene units are organized highly contracted and helically coiled gauche-gauche conformation. Along with chemical stability and stain resistance, PTT possesses much small crystal modulus of 2.59 GPa with strong flexibility and more than 90% elastic recovery [13–17]. Its relatively large refractive index (1.638) [18] than that of silica (1.46), fluoride glass (1.48), phosphate glass (1.54), poly(methyl methacrylate) (1.54), and polystyrene (1.59), provides fine optical confinement. PTT nanofibrous mats with diameters of 200–600 nm have been fabricated by electrospinning [19]. However, the nanofiber fabricated by electrospinning with large surface roughness and length inhomogeneity induces high optical loss. Recently, absorption properties of PTT material have been studied in infrared region [20]. To further explore PTT's optical characteristics and its applications in nanophotonic devices, here we found that PTT exhibits good transparency from visible lights to near-infrared and fine performance for advanced nanofibers and nanophotonic devices.

2. PTT nanofiber fabrication

Using direct drawing technique, PTT nanofiber with diameters down to 60 nm and lengths up to 500 mm were fabricated by one-step process as described in Fig. 1. We use a heating plate to melt PTT pellets (melt temperature $T_m = 225^\circ\text{C}$) [16] and keep temperature at around

250°C during the fiber drawing. First, an iron or silica rod with radius of about 125 μm is being approached and its tip is immersed into the molten PTT. Then the rod tip is retracted from the molten PTT with a speed of 0.1–1 m/s, leaving a PTT wire extending between the molten PTT and the tip. The extended PTT wire is quickly quenched in air and finally, a naked amorphous PTT nanofiber is formed.

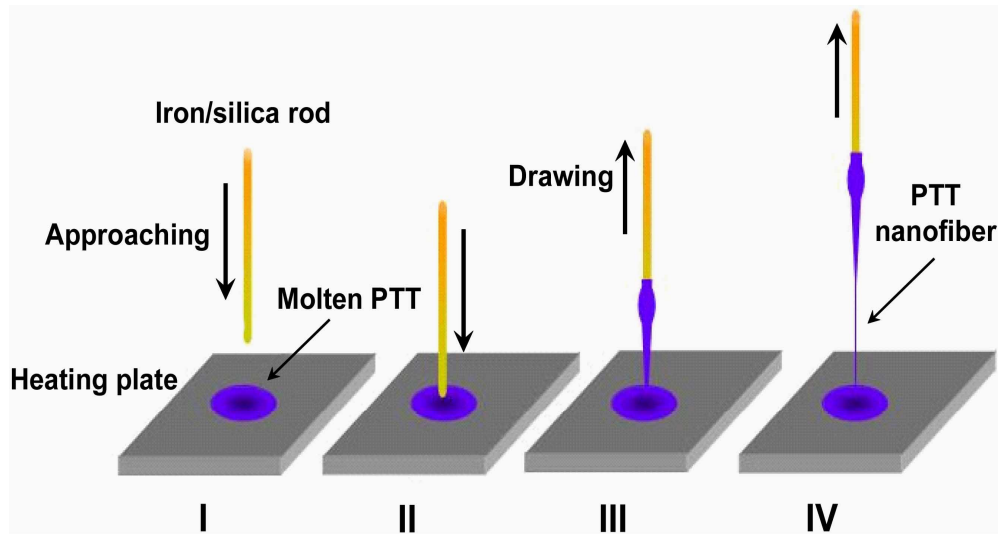


Fig. 1. Schematic illustration of nanofibers fabrication by direct drawing process from molten PTT. I, An iron or silica rod is approaching the molten PTT. II, The rod end is immersed into the molten PTT. III, The rod conglutinated PTT is being drawn out. IV, A PTT nanofiber is formed.

3. Devices assembly and characterization

To display the fabricated PTT nanofiber, we coiled a 250-mm-long PTT nanofiber on a 12- μm -diameter PTT bending rod. A scanning electron microscope (SEM) image (Fig. 2(a)) shows part of the coiled nanofiber with a length of about 200 mm and an average diameter of 280 nm. The diameter variation ratio is about 8.4×10^{-8} . To examine surface roughness of the nanofibers, a high-magnification transmission electron microscope (TEM) was done. Figures 2(b) and 2(c) show TEM images of a 70-nm-diameter nanofiber and of the sidewall of a 180-nm-diameter nanofiber, respectively, indicating that there is no visible defect and irregularity in the surface of the nanofibers. Typically, the average sidewall root-mean-square roughness of these nanofibers is 0.28 nm. The electron diffraction pattern (the inset of Fig. 2(c)) demonstrates that the PTT nanofiber is amorphous. The PTT nanofibers have highly configurable capability that can be easily and repeatedly manipulated to fashion a variety of shapes. For the further study, we use a micro-manipulator to cut, position, bend, twist, and pull the nanofibers with high precision under an optical microscope. Flexible rings with respective bending radius as small as 250 and 700 nm were formed by positioning a 105-nm-diameter nanofiber (Fig. 2(d)). The nanofibers can also be bent from 0 to 180°, as an example, Fig. 2(e) shows a 155° sharp bend with diameter of 160 nm. Figure 2(f) shows that a 340-nm-diameter nanofiber was bent to a tweezer-shaped structure with a bending radius of 1.6 μm . Similarly, a 70-nm-diameter nanofiber was first twisted, and then bent to form a scissor-shaped structure (Fig. 2(g)). Figure 2(h) shows a 2×2 coupler with three twist turns in the coupling region by twisting 110-nm- and 150-nm-diameter nanofibers. Figure 2(i) demonstrates flexible and elastic connections by pulling the nanofibers with diameters of 140 and 170 nm. Furthermore, the nanofibers can be easily and repeatedly manipulated to form a variety of shapes with nondestructive. The nanofibers with high surface smoothness, diameter

uniformity, as well as good excellent flexibility, make them promising candidates for constructing ultracompact photonic devices and device arrays.

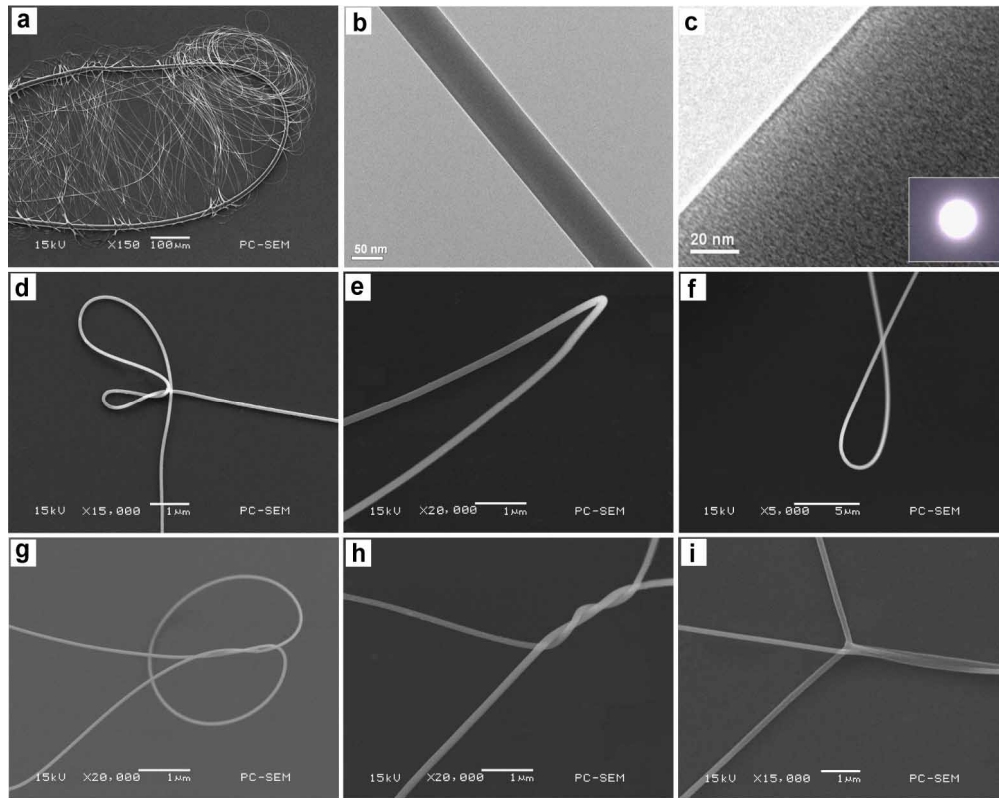


Fig. 2. Electron micrographs of PTT nanofibers and nanofiber structures. (a),(d)–(i), Scanning electron microscope (SEM) images; (b), (c) Transmission electron microscope (TEM) images. (a) A nanofiber with average diameter of 280 nm coiled on a 12- μ m-diameter PTT bending rod, the length of the nanofiber displayed is about 200 mm. (b) A 70-nm-diameter PTT nanofiber. (c) The surface of a 180-nm-diameter nanofiber and the electron diffraction pattern (inset). (d) 105-nm-diameter flexible nanofiber rings. (e) A 155° sharp bend with a diameter of 160 nm. (f) A 340-nm-diameter tweezer-shaped nanofiber. (g) A 70-nm-diameter scissor-shaped nanofiber. (h) A twisted 2 \times 2 coupler consists of 110-nm- and 150-nm-diameter nanofibers. (i) Flexible and elastic enough nanofiber connection with diameters of 140 and 170 nm.

Figure 3 shows the SEM images of some nanofiber devices and device arrays. Figure 3(a) shows a directional coupler assembled by two parallel 750-nm-diameter nanofibers with a 110 nm coupling gap. Figure 3(b) shows a Y-branching coupler assembled by two 360-nm-diameter nanofibers without coupling gap. We further assembled a bending Y-branching coupler by a 210-nm-diameter 155° bend (inside up) and a 270-nm-diameter 120° bend (outside down) (Fig. 3(c)), a 2 \times 2 coupler by two 150-nm-diameter nanofibers (Fig. 3(d)), and a basic asymmetric MZ coupler by two 60-nm-diameter nanofibers (Fig. 3(e)). Furthermore, integrated device arrays were constructed (Figs. 3(f)–3(i)), where the insets in yellow colour show their respective schematic structures. Figure 3(f) shows an integrated structure cascaded by two MZ couplers using 100-nm-diameter nanofibers. Figure 3(g) shows an integrated device cascaded by a 2 \times 2 coupler and a MZ coupler using 130-nm-diameter nanofibers. Figure 3(h) shows a three inputs four outputs device array formed by two 300-nm-diameter 2 \times 2 couplers in parallel and, Fig. 3(i) shows a three inputs three outputs device array formed by four X-crosses with nanofiber diameter of 560 nm.

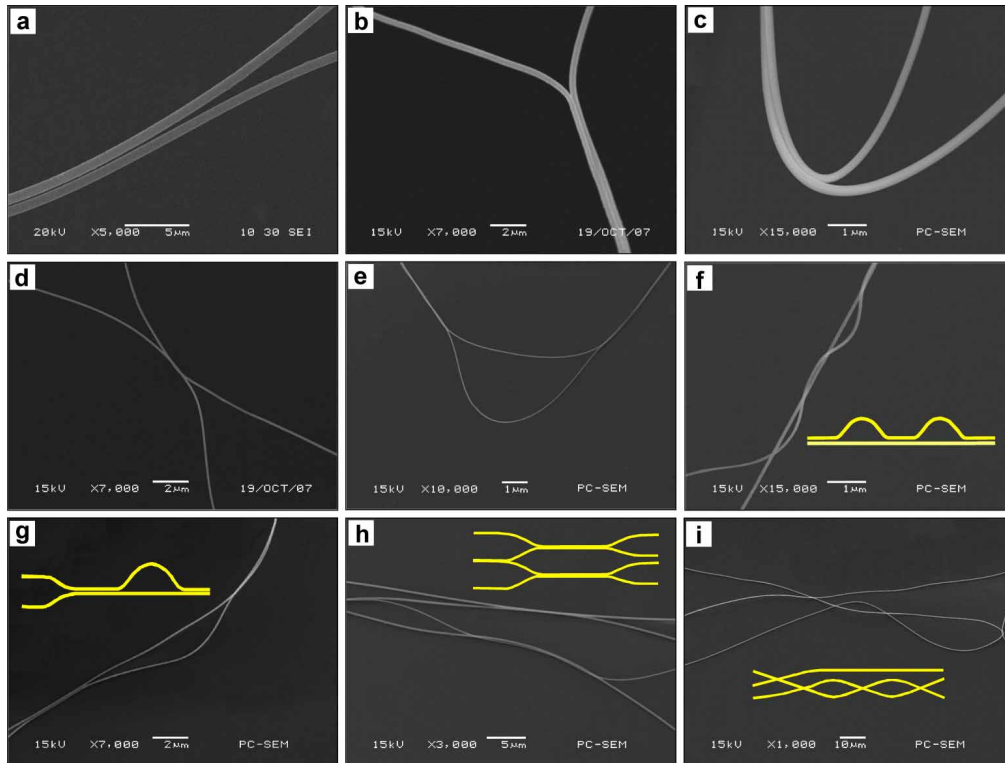


Fig. 3. SEM images of photonic devices and device arrays constructed by PTT nanofibers. (a) A directional coupler with a 110 nm coupling gap between the two 750-nm-diameter nanofibers. (b) A 360-nm-diameter Y-branching coupler without coupling gap. (c) A zero coupling gap coupler cascaded by a bending Y-branch (inside bend: 155°-bending-angle, 210-nm-diameter; outside bend: 120°-bending-angle, 270-nm-diameter). (d) A 2×2 coupler (150-nm-diameter). (e) A basic asymmetric MZ structure (60-nm-diameter). (f) An integrated coupler cascaded by two MZ structures (100-nm-diameter). (g) An integrated device cascaded by a 2×2 coupler and a MZ structure (130-nm-diameter). (h) A three inputs four outputs device array integrated by two 2×2 couplers (300-nm-diameter). (i) A three inputs three outputs device array integrated by four X-crosses (560-nm-diameter). The insets in yellow colour in (f)–(i) show respective schematic diagrams of the integrated structures.

4. Optical coupling and loss measurement

To investigate guided optical properties of the PTT nanofibers and the devices, we fixed the nanofibers and/or nanofiber devices by two microstage supports, and launched lights of different wavelength into the structures by evanescent coupling through directional coupling as shown in Fig. 4(a). As an example, the figure shows green light (532 nm) was coupled into a 470-nm-diameter PTT nanofiber bend from a submicro-taper silica fiber with a coupling length of 10.5 μm , where the upper red and yellow colors show the simulated evanescent coupling by the beam propagation method (BPM). It should be emphasized that some light scattering in the PTT nanofiber was induced by surface contamination rather than surface roughness. The output powers from the PTT nanofibers were measured by an optical power meter together with an optical spectrum analyzer. The optical losses of the PTT nanofibers were measured by a cutback method. In the measurement, the original nanofiber we used to evaluate the loss is 5 to 20 cm. In each cutback of the measurement, about 1-mm-long fiber was cut off from the output end of the nanofiber. Figure 4(b) shows the plots of the PTT fiber diameter versus measured optical loss at the wavelengths of 473, 532, 650, 1310, and 1550 nm, and the inset shows the transmittance of $\sim 90\%$ in the wavelength region of 400 to 2000

nm for a 25- μm -thick amorphous PTT film. The measured rate of the PTT nanofibers' loss over time is 0.4 dB/hour, which is smaller than that of the silica nanowires (about 1 dB/hour) [7].

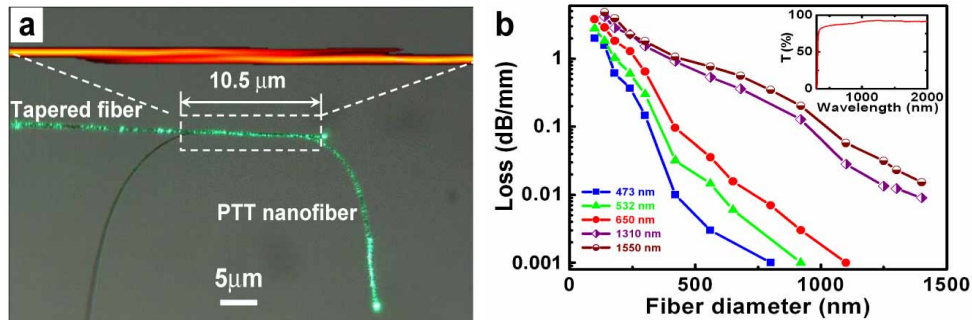


Fig. 4. Optical coupling method and the measured optical loss. (a) Optical microscope image of a tapered silica fiber launched 532 nm green light into a 470-nm-diameter PTT nanofiber bend by evanescent coupling, where the coupling length is 10.5 μm . The upper red and yellow colors illustrate the coupling region simulated by the beam propagation method. (b) Optical loss of PTT fiber versus different diameter at the wavelengths of 473, 532, 650, 1310, and 1550 nm. The inset shows the transmission spectrum for a 25- μm -thick amorphous PTT film.

5. Optical characterization of device and device arrays

In characterization, optical signals were coupled into the PTT nanofibers by evanescent coupling as shown in Fig. 4(a) and the measured optical losses were plotted in Fig. 4(b). Subsequently, to analyze the optical characteristics at different wavelengths, we launched lights of different wavelengths into the assembled nanofiber devices and device arrays. As an example, Fig. 5(a) shows the launched blue light (473 nm) in the input port B is split into two parts by a 2 \times 2 branching splitter, which was formed by twisting two 340-nm-diameter nanofibers with one twist turn. The twisted region is shown in the inset of Fig. 5(a). The branching angles is 25 $^\circ$ and the splitting ratio is 46:54 for the outputs C:D. The measured insertion loss is less than 0.3 dB. We have also assembled a 1 \times 3 branching splitter by twisting three 290-nm-diameter nanofibers (Fig. 5(b)), and coupled blue light into the input port A with a splitting ratio of about 35:40:25 (from output ports B to D) and a total insertion loss of less than 0.3 dB. Figure 5c further shows red light (650 nm) in a 1 \times 4 branching splitter with diameter of 350nm and splitting ratio of 23:20:28:29 (from output ports B to E). The measured total insertion loss is about 0.35 dB. From Figs. 5(a)–5(c), we can see that the scattering lights are extremely weak in the branching areas, which is desirable for high performance optical beam splitters/couplers. In Fig. 5(d), we launched red light into a 500-nm-diameter twisted spiral nanofiber with a 680-nm-radius ring at its end and found that that the optical power was well confined within the fiber core. BPM analysis shows that the bending loss is about 0.15 dB through the nanoring with radius as small as 680 nm, which is smaller than that of silica nanowires [9]. Figure 5(e) shows green light in an 850-nm-radius ring with nanofiber diameter of 120 nm. The result shows that the optical field is confined in a small area of about 0.3 μm \times 0.3 μm around the nanofiber with good optical confinement. Our results can be compared with that of a SnO₂ nanoribbon S turn (dimensions of 785 μm by 275 nm by 150 nm) with curvature as small as 1 μm [2]. In addition, the studies of Barrelet *et al.* have illustrated optical guiding properties through sharp bends in 100-nm-diameter CdS nanowires structure [21]. We have also characterized a 230-nm-diameter racetrack-shaped resonator (Fig. 5(f)), which exhibits good transmission with an insertion loss of about 1.0 dB. In addition to above, optical microscope image of our double-loop resonator (550-nm-diameter) with an average radius of about 3.8 μm (Fig. 5(g)) demonstrates that light can also be transmitted in multiple-rings (the measured total insertion loss is 2.4 dB). Therefore, a

variety of ring-typed structures, ranging from simple fiber knot to complex coil/microcoil resonators [22,23] can be achieved by proper assembling of the PTT nanofibers. Figure 5(h) shows blue light in a 210-nm-diameter integrated structure cascaded by a basic asymmetric MZ structure and an 850-nm-radius ring. The total insertion loss is 0.38 dB. Moreover, Fig. 5(i) shows blue light in a 210-nm-diameter integrated structure cascaded by two basic asymmetric MZ couplers with a total insertion loss of 0.33 dB. These structures demonstrate good feasibility of PTT nanofiber-based integrated devices for miniaturized photonic integrated circuits.

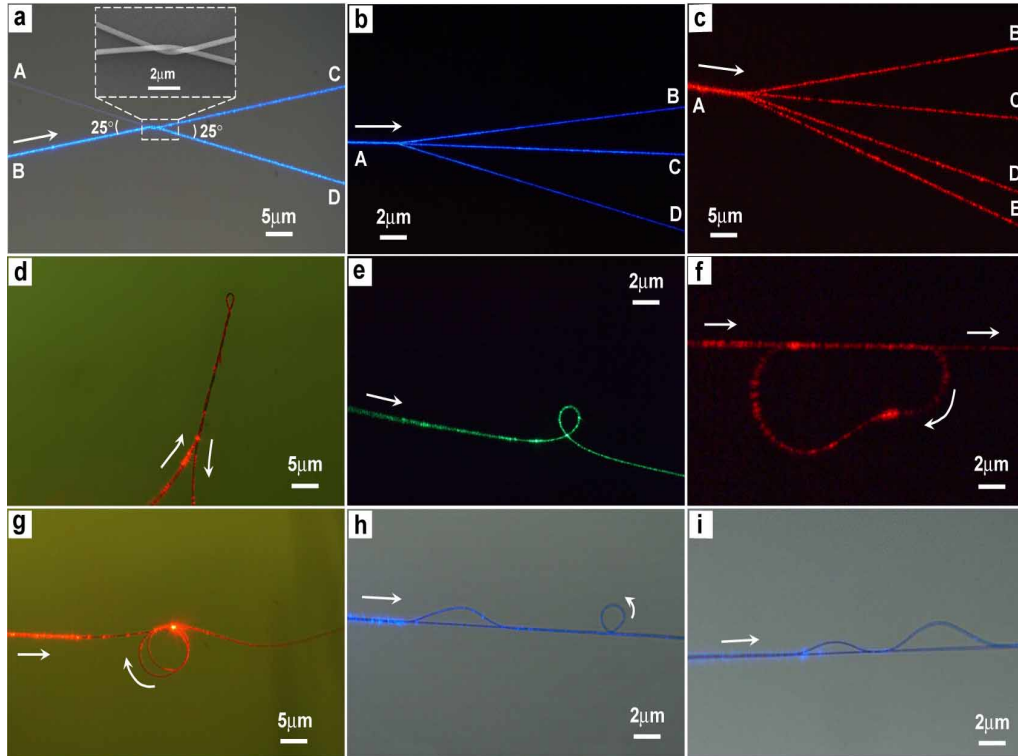


Fig. 5. Optical microscope images of the guided visible lights in different PTT nanofibers and nanofiber devices. (a) Blue light in a 2×2 (340-nm-diameter) branching splitter. (b) Blue light in a 1×3 (290-nm-diameter) branching splitter. (c) Red light in a 1×4 (350-nm-diameter) branching splitter. (d) Red light in a 500-nm-diameter twisted spiral nanofiber with a 680-nm-radius ring. (e) Green light in an 850-nm-radius ring (120-nm-diameter). (f) Red light in a 230-nm-diameter racetrack-shaped resonator. (g) Red light in a 550-nm-diameter doubled-loop resonator (average radius about 3.8 μm). (h) Blue light in a 210-nm-diameter integrated device cascaded by a MZ structure and an 850-nm-radius ring. (i) Blue light in an integrated structure cascaded by two MZ structures (210-nm-diameter).

6. Conclusion

In summary, PTT nanofibers with diameters down to 60 nm and lengths up to 500 mm have been drawn by the one-step direct drawing technique. The nanofibers exhibit high surface smoothness, length uniformity, and mechanical strength. PTT nanofiber devices including optical beam splitters, couplers, nanorings, tweezer/scissor-shaped structures, and a series of nanophotonic device arrays have been assembled and demonstrated. The results show that the PTT fiber reported here opens up an avenue for novel optical fibers for wavelengths ranging from visible to near infrared, and they can be arbitrarily positioned, bent, intertwined, twisted, tensed, and assembled into different structures. By adopting photosensitive materials such as rare-earth into the molten PTT, one might draw more versatile nanofibers and photonic

devices by this technique. We expect the PTT material, nanofibers, nanofiber devices, and the one-step fabrication technology may find wide applications in integrated optics and PICs.

Acknowledgments

This work was supported by the National Natural Science Foundation of China (Grant Nos. 60625404, 60577001). The authors thank Prof. Xudong Chen for material supply, Wen He, Heng Zhu, Weiang Luo, and Like Lu for assistance in samples preparation, Prof. Yuezhong Meng for assistance in SEM measurements, Menglin Guo and Jinchun Shi for assistance in optical coupling. The authors acknowledge Prof. Bharat S. Chaudhari (Ph.D.) from International Institute of Information Technology, Pune, India, for his assistance and fruitful discussion.